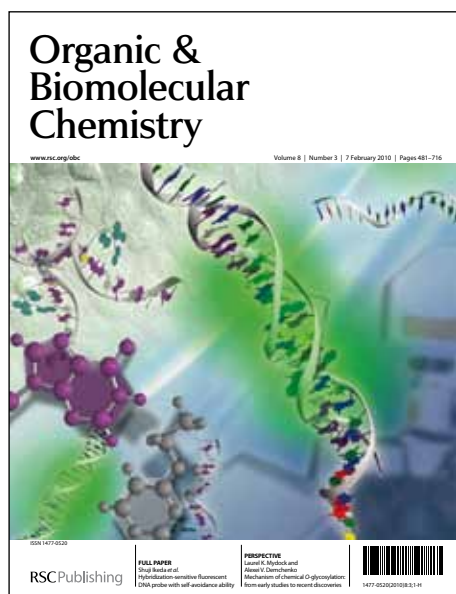


Organic & Biomolecular Chemistry

Accepted Manuscript

This article can be cited before page numbers have been issued, to do this please use: A. J. Kirby, F. Nome, M. Medeiros, E. H. Wanderlind, J. R. Mora and R. Moreira, *Org. Biomol. Chem.*, 2013, DOI: 10.1039/C3OB40988K.



This is an *Accepted Manuscript*, which has been through the RSC Publishing peer review process and has been accepted for publication.

Accepted Manuscripts are published online shortly after acceptance, which is prior to technical editing, formatting and proof reading. This free service from RSC Publishing allows authors to make their results available to the community, in citable form, before publication of the edited article. This *Accepted Manuscript* will be replaced by the edited and formatted *Advance Article* as soon as this is available.

To cite this manuscript please use its permanent Digital Object Identifier (DOI®), which is identical for all formats of publication.

More information about *Accepted Manuscripts* can be found in the [Information for Authors](#).

Please note that technical editing may introduce minor changes to the text and/or graphics contained in the manuscript submitted by the author(s) which may alter content, and that the standard [Terms & Conditions](#) and the [ethical guidelines](#) that apply to the journal are still applicable. In no event shall the RSC be held responsible for any errors or omissions in these *Accepted Manuscript* manuscripts or any consequences arising from the use of any information contained in them.

Major mechanistic differences between the reactions of hydroxylamine with phosphate di- and tri-esters

View Article Online
DOI: 10.1039/C3OB40988K

Michelle Medeiros[†], Eduardo H. Wanderlind[†], José R. Mora[†], Raphaell Moreira[†], Anthony J. Kirby^{,§} and Faruk Nome^{*,†}.*

[†] Instituto Nacional de Ciência e Tecnologia (INCT) de Catálise, Departamento de Química, Universidade Federal de Santa Catarina (UFSC), CEP 88040-900, Florianópolis, Santa Catarina (SC), Brazil. [§] University Chemical Laboratory, Cambridge CB2 1EW, UK.

* Corresponding authors' email addresses: faruk.nome@ufsc.br; ajk1@cam.ac.uk

Invited contribution for the birthday celebration issue for Andy Hamilton

Abstract: Hydroxylamine reacts as an oxygen nucleophile, most likely via its ammonia oxide tautomer, towards both phosphate di- and triesters of 2-hydroxypyridine. But the reactions are very different. The product of the two-step reaction with the triester **TPP** is trapped by the NH_2OH present in solution to generate diimide, identified from its expected disproportionation and trapping products. The reaction with $\text{H}_3\text{N}^+-\text{O}^-$ shows general base catalysis, which calculations show is involved in the breakdown of the phosphorane addition-intermediate of a two-step reaction. The reactivity of the diester anion **DPP⁻** is controlled by its more basic pyridyl N. Hydroxylamine reacts preferentially with the substrate zwitterion **DPP[±]** to displace first one then a second 2-pyridone, in concerted $\text{S}_{\text{N}}2(\text{P})$ reactions, forming O-phosphorylated products which are readily hydrolysed to inorganic phosphate. The suggested mechanisms are tested and supported by extensive theoretical calculations.

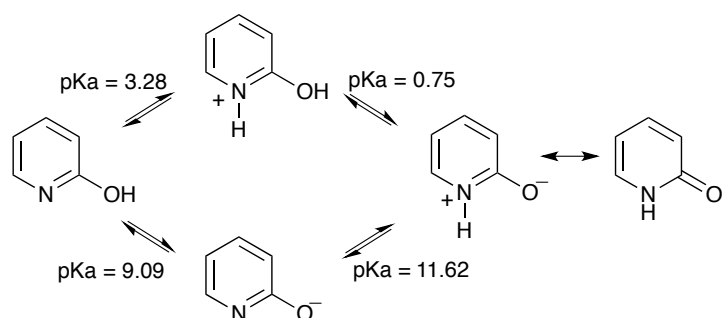
View Article Online
DOI: 10.1039/C3OB40988K

Keywords:

Phosphate transfer mechanism; ammonia oxide; α -nucleophile.

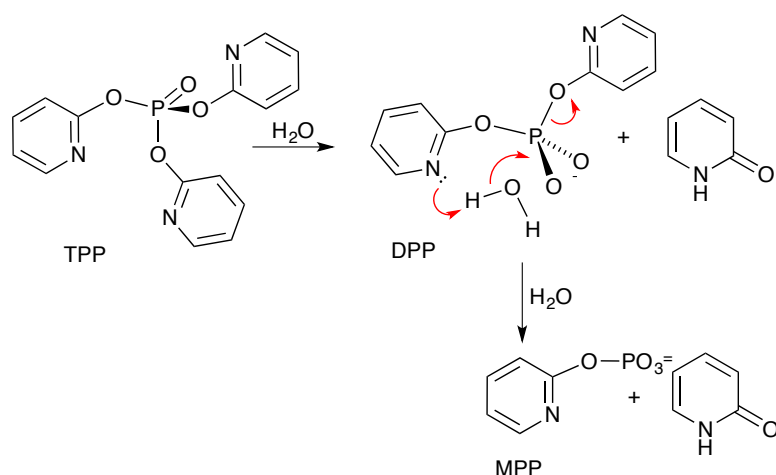
Introduction

Phosphoryl transfer reactions are involved in countless essential biochemical processes, not least the storage and transmission of genetic information. Extensive studies focused on detailed mechanistic descriptions of simple models of nucleophilic substitutions in phosphate esters have been summarised in recent reviews.¹⁻³ For four decades the reactivity of phosphate esters has been evaluated almost exclusively in terms of nucleophile and leaving group capabilities, and a wide range of data, particularly linear free energy relationships (LFERs), has been reported for nucleophilic substitution reactions of phosphate mono-, di- and triesters.⁴⁻⁸ We have investigated the mechanisms of reactions of nucleophiles (always including water) with a broad range of phosphate esters, typically featuring alkyl and substituted-phenyl substituents:^{9, 10} and most recently for pyridyl esters.^{11, 12} This latter work was prompted by the intriguing report of Liu and Wulff that an attempted preparation of di-2-pyridyl phosphate **DPP** "failed owing to its instability".¹³ This was intriguing because diesters are known as the least reactive esters of phosphoric acid (for example, the half-time for the spontaneous hydrolysis of diphenyl phosphate at 100°C is an estimated 180 years.⁶) And has led to a series of studies on the reactions of phosphate esters with 2-hydroxypyridine (Scheme 1) as leaving group. These are conveniently summarised in the most recent report, on the hydrolysis of **DPP** itself.¹¹



Scheme 1. Equilibria and pK_a values for 2-hydroxypyridine: which exists in water almost exclusively as 2-pyridone.¹⁴

2-Hydroxypyridine, with a pK_a of 9.09, exists in water almost exclusively as 2-pyridone (Scheme 1), and its anion is expected to be a poor leaving group. The **DPP**⁻ anion is indeed hydrolysed very slowly, with a half-life of 70 years at 25°C.¹¹ Nevertheless, this is many thousands of times faster than expected for a diester with leaving groups of pK_a 9.09, and we have proposed that this is the result of efficient intramolecular general base catalysis by the pyridine nitrogen of the non-leaving group (Scheme 2).¹¹ Interestingly, no intramolecular catalysis was apparent for the hydrolysis of the much more reactive triester, **TPP** (Scheme 2): which has considerably less basic pyridines.



Scheme 2. The hydrolysis reactions of neutral **TPP** and anionic **DPP**.^{11, 15}

This published work involves contrasting reactions of two related phosphate esters, **TPP** and **DPP**, which show very different reactivities towards one of the weakest oxygen nucleophiles, and we were interested to see how they fared when challenged by one of the strongest. The strongest nucleophile in water is the anion of NH₂OH, but the pK_a of 13.42 for the OH group means that the anion is present only at very high pH. However, hydroxylamine can itself be a remarkably reactive "α-nucleophile"¹⁶ towards phosphate phosphorus, reacting through oxygen via its ammonia oxide tautomer H₃N⁺-O⁻,¹⁶ which makes up almost 20% of a

solution of hydroxylamine in water.¹⁷ We present a full mechanistic investigation involving kinetic, NMR, ESI-MS and theoretical calculations, comparing the reactions of hydroxylamine with **TPP** and **DPP**: which turn out to be very different.

View Article Online
DOI: 10.1039/C3OB40988K

Results and discussion

Reaction of TPP with hydroxylamine

Kinetics. Reactions were followed spectrophotometrically in aqueous media by monitoring the appearance of the product 2-pyridone at 294 nm, using an excess of hydroxylamine to ensure that reactions were pseudo-first order with respect to the substrate. The pH-rate profile for the reaction (upper curve of Figure 1) shows that k_{obs} increases with increasing pH between 4 – 8, consistent with neutral hydroxylamine ($\text{NH}_2\text{OH} \rightleftharpoons \text{H}_3\text{N}^+\text{O}^-$) as the reacting species (the $\text{p}K_{\text{a}}$ of acid dissociation of $^+\text{NH}_3\text{OH}$ is 6.06).

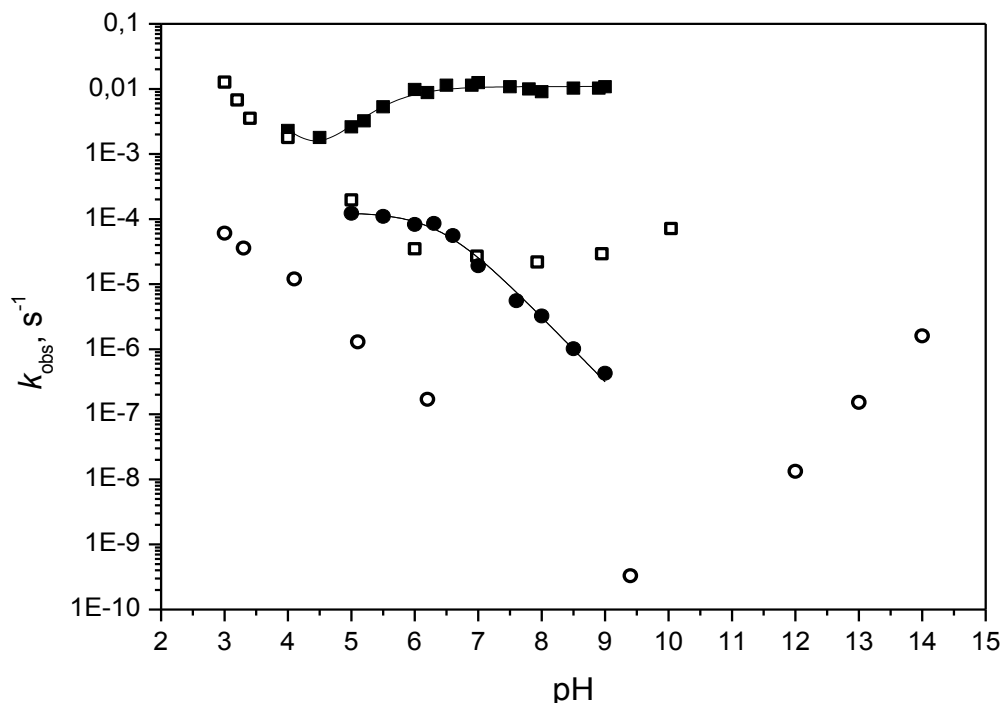


Figure 1. pH-rate profiles for the reactions of **TPP** with 0.5M NH_2OH (■), and **DPP** with 1M

NH₂OH (●), both at 25°C and *I*=1.0 (KCl). Data for the spontaneous hydrolyses of **TPP** (□) and **DPP** (○) at 25°C, studied previously,^{11, 15} are shown for comparison.

View Article Online
DOI: 10.1039/C3OB40988K

The disappearance of **TPP** in the presence of 0.5M hydroxylamine is some 400 times faster than its spontaneous hydrolysis at pH 8 (on the plateau regions of the profiles shown in Figure 1), consistent with the expected rapid nucleophilic reaction with hydroxylamine. However, a plot of k_{obs} vs hydroxylamine concentration (Figure 2) shows linear behavior only at very low concentrations of the nucleophile, with the marked curvature at higher [NH₂OH] evidence for a reaction second order in hydroxylamine.

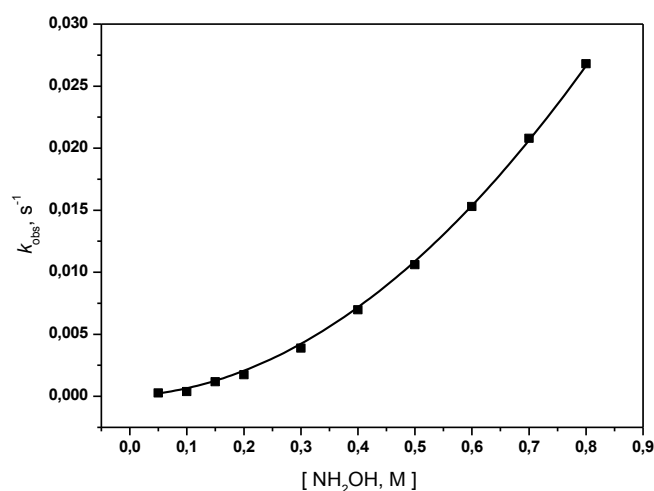
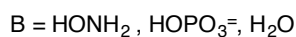
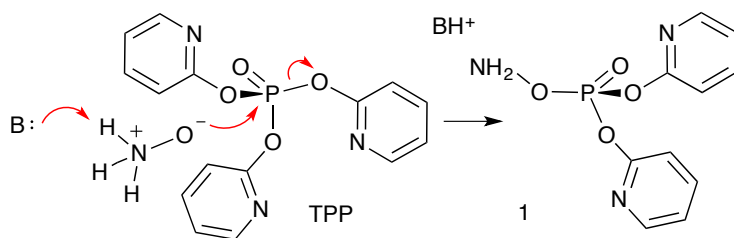


Figure 2. Dependence of k_{obs} on hydroxylamine concentration in the reaction with **TPP** at 25°C, pH 8.5 and *I*=1.0 (KCl). The solid line represents the curve fit to equation (1): $k_{\text{obs}} = k_0 + k_2[\text{NH}_2\text{OH}] + k_3[\text{NH}_2\text{OH}]^2$. Results appear in Table 1.

The (upper) profile of Figure 1 is thus accounted for by pathways both first and second order in hydroxylamine, which make the major contributions to k_{obs} at low and high [NH₂OH], respectively. (Calculated rate enhancements over k_0 for 1M hydroxylamine are 106-fold for the second order (k_2) reaction, and 1638-fold for the competitive (k_3) path involving two

hydroxylamine molecules.) Only one molecule can act as the nucleophile, so the second hydroxylamine acts, at least kinetically, as a general base. Hydroxylamine itself has no special properties as a base, so as a simple test to verify general base catalysis of the reaction, we looked for – and found – comparable buffer catalysis by dipotassium hydrogen phosphate, which has a similar pK_a . The second order rate constant for buffer catalysis by K_2HPO_4 of the reaction with 0.1M NH_2OH is $3.82 \times 10^{-3} M^{-1} s^{-1}$ compared with $3.85 \times 10^{-2} M^{-1} s^{-1}$ for catalysis by the second molecule of (1M) hydroxylamine. (The data are shown in Table S.2 of the Supporting Information).

These results are consistent with the general base assisting nucleophilic attack by hydroxylamine, as in Scheme 3: or alternatively with catalysis of the second step of a reaction involving a pentacovalent intermediate. There is general agreement that the hydrolysis of phosphate triesters is a two-step process, and indications that the second step may become rate-determining for the reactions of triaryl esters.¹⁸



Scheme 3. Single-step mechanism (see the text) for the reaction of hydroxylamine with **TPP** to form the O-phosphorylated derivative (**1**). Solvent may be presumed to act as the general base for the first order reaction. The evidence favouring ammonia oxide as the active nucleophile is discussed below.

The full pH-rate profile (Figure 1) for the reaction with **TPP** with 0.5M hydroxylamine was fitted to equation (2) [based on eq. (1), Figure 2: but including also terms for the reactions of the conjugate acid **TPPH⁺** (protonated on pyridyl nitrogen)].

View Article Online
DOI: 10.1039/C3OB40988K

$$k_{\text{obs}} = k_{\text{H}} \cdot \chi_{\text{TPPH}^+} + \left[k_0 + k_2 [\text{NH}_2\text{OH}] \cdot \chi_{\text{NH}_2\text{OH}} + k_3 ([\text{NH}_2\text{OH}] \cdot \chi_{\text{NH}_2\text{OH}})^2 + k_4 [\text{NH}_2\text{OH}]^2 \cdot \chi_{\text{NH}_2\text{OH}} \cdot \chi_{\text{NH}_3\text{OH}^+} \right] \cdot \chi_{\text{TPP}} \quad (2)$$

Here $\chi_{\text{NH}_2\text{OH}}$, $\chi_{\text{NH}_3\text{OH}^+}$, χ_{TPP} and χ_{TPPH^+} are the molar fractions of neutral hydroxylamine, NH_3^+OH , neutral **TPP** and **TPPH⁺**. The parameters obtained from the least squares fit appear in Table 1. The hydrolysis rate constant k_{H} makes the major contribution to k_{obs} at lower pHs: k_4 , we take to represent the kinetically equivalent reaction of **TPPH⁺**, second order in NH_2OH : corresponding to the mechanism of Scheme 3 but with neutral 2-pyridone as the leaving group. Full details of the analysis and curve-fitting appear in the Supporting Information.

Table 1. Kinetic parameters for reactions of hydroxylamine with **TPP** in water.^a

$k_{\text{H}}, \text{s}^{-1} \text{ }^{\text{b}}$	36.5±13.3
$k_0, \text{s}^{-1} \text{ }^{\text{b}}$	2.35x10 ⁻⁵
$k_2, \text{M}^{-1} \text{s}^{-1} \text{ }^{\text{c}}$	2.50 x 10 ⁻³
$k_3, \text{M}^{-2} \text{s}^{-1} \text{ }^{\text{c}}$	3.85 x 10 ⁻²
$k_4, \text{M}^{-2} \text{s}^{-1}$	(1.03±0.07)x10 ⁻¹
$\text{p}K_{\text{a}} (\text{TPPH}^+) \text{ }^{\text{b}}$	-0.22
$\text{p}K_{\text{a}} (\text{NH}_3\text{OH}^+) \text{ }^{\text{b}}$	6.06

^a First, second and third order rate constants were obtained by fitting the pH-rate profile (Figure 1) to eq. 2. ^b Data from the literature.^{15,19} ^c k_2 and k_3 values obtained by fitting the profile of k_{obs} vs. $[\text{NH}_2\text{OH}]$ (Figure 2) to eq. 1.

We showed in previous work that almost 20% of hydroxylamine exists in aqueous solution as the zwitterion ammonia oxide ($^+\text{NH}_3\text{O}^-$),¹⁷ a highly reactive nucleophile towards the phosphoryl centre, of triesters in particular.¹⁶ We have tested the mechanism by measuring the solvent kinetic isotope effect (SKIE) for the reaction. In the presence of 0.5M hydroxylamine, at pH(D) 8.5, where the reaction is carried almost entirely (94%) by the third order process, we observe a SKIE, $k_{\text{H}_2\text{O}}/k_{\text{D}_2\text{O}}$, of 1.7. This is consistent with the involvement of proton transfer in the transition state, and thus (though not uniquely) consistent with a general base catalysis mechanism such as that suggested in Scheme 3.

View Article Online
DOI: 10.1039/C3OB40988K

More specific information comes from a proton inventory study, conducted under the same conditions for the pH-independent reaction of 0.5M hydroxylamine with **TPP** at 25.0 °C, pH 8.5 (TRIS buffer, 0.01 mol L⁻¹, 1 mol L⁻¹ KCl). The solvent isotope effect in mixtures of HOH ($n = 1 - 0$) and DOD ($n = 0 - 1$) shows a curved dependence of k_n/k_0 on the atom fraction n of deuterium (Figure S.3a in the Supporting Information). For a reaction between a phosphate triester such as **TPP** (without exchangeable hydrogens) and ammonia oxide, we can reasonably expect the fractionation factors of the reagents (ϕ_i^{R}) to be close to unity. Accordingly, the data give an acceptable fit ($R^2 = 0.989$) to the Gross-Butler equation in its simplified form (Eq. 4):

$$k_n = k_{\text{H}}(1 - n + n \cdot \phi_i^{\text{T}})^m \quad \text{Eq. 4}$$

with a fractionation factor $\phi_i^{\text{T}} = 0.87$ and a value of $m = 3.6$, suggesting that there are some 3 – 4 protons in-flight in the rate determining transition state. Since the isotope effect is not very large, we decided to test if the proton inventory could be reasonably fitted with two in-flight protons. The plot of $(k_n/k_{\text{H}})^{1/2}$ versus $n_{\text{D}_2\text{O}}$ (Figure S.3b) was linear with $R = 0.994$ and the expected intercept of unity (0.997 ± 0.007) and slope = -0.227 ± 0.011 are consistent with two mobile hydrogens with a fractionation factor $\phi_i^{\text{T}} = 0.773$. Since the two results are statistically

equivalent, we apply Occam's razor, and conclude that the proton inventory study favours a transition state with *at least two* hydrogens in-flight.

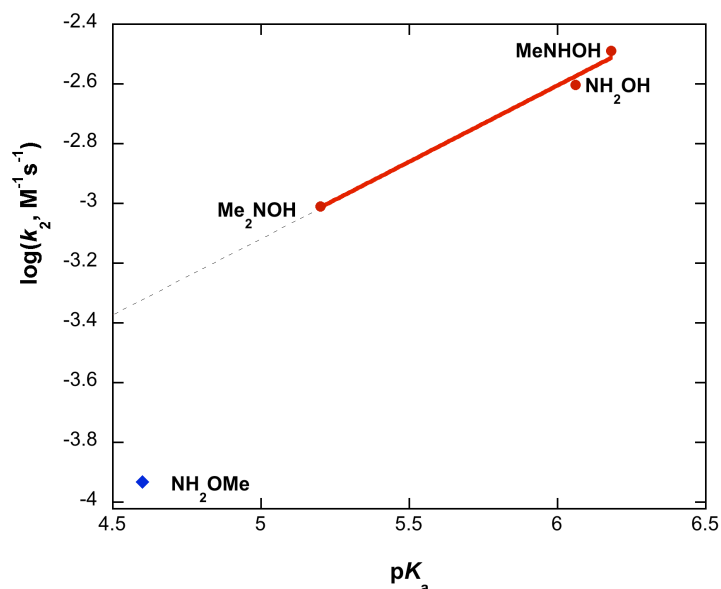
View Article Online
DOI: 10.1039/C3OB40988K

To confirm that hydroxylamine acts predominantly as an oxygen nucleophile, we followed the reactions of **TPP** with its N- and O-methyl hydroxylamine derivatives: and found different behavior for different potential nucleophiles. The rate-concentration profile for the reaction with *N*-methyl hydroxylamine is similar to that of hydroxylamine in showing a second order component: while those for *N,N*-dimethyl hydroxylamine and *O*-methyl hydroxylamine do not (the three profiles are shown in Figure S.2 of the Supporting Information). Since the reaction of **TPP** with Me₂NOH is already 12 times slower than with hydroxylamine itself, we presume that the third order term for general base catalysis by the considerably less basic dimethylamino compound is simply too slow to be significant at the highest concentration (0.3M) used. Second and (where applicable) third order rate constants obtained for each nucleophile are presented in Table 2, together with their p*K*_a values: which are used in the Brønsted plot of Figure 3.

Table 2. Rate constants for reactions of **TPP** with hydroxylamine and its derivatives, all at 25°C, pH=8.5 and *I*=1.0 (KCl).^{a,b}

Nucleophile	p <i>K</i> _a	<i>k</i> ₂ , M ⁻¹ s ⁻¹	<i>k</i> ₃ , M ⁻² s ⁻¹
NH ₂ OH	6.06	2.50 x 10 ⁻³	3.85 x 10 ⁻²
MeNHOH	6.18	3.25 x 10 ⁻³	1.51 x 10 ⁻²
NMe ₂ OH	5.20	9.78 x 10 ⁻⁴	-
NH ₂ OMe	4.60	1.17 x 10 ⁻⁴	-

^a Rate constants were obtained by fitting the rate-concentration profiles, see Figure S.2 of the Supporting Information (the plot of *k*_{obs} vs. [NH₂OH] is shown in Figure 2, above). ^b p*K*_a values were obtained from literature.¹⁹



View Article Online
DOI: 10.1039/C3OB40988K

Figure 3. Brønsted plot for the (first-order) reactions of **TPP** with hydroxylamine nucleophiles, at 25°C.

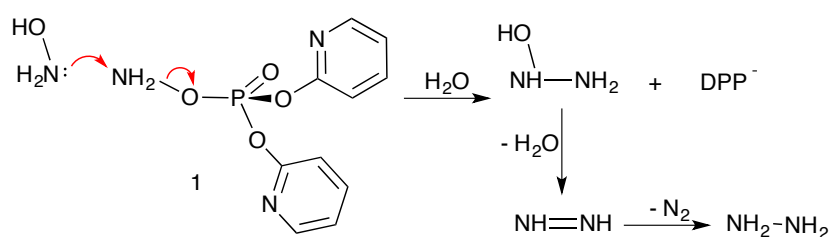
The rate constants in Table 2 show that **TPP** reacts more slowly with less basic hydroxylamines, as expected: but the Brønsted plot of Figure 3 shows that NH_2OMe does not fit the relationship accurately defined by the points for hydroxylamine and its mono- and di-*N*-methyl derivatives, but reacts 4-5 times more slowly than expected from the correlation. This behavior is precedented,²⁰ and consistent with hydroxylamines with N–OH groups acting as oxygen nucleophiles in their reactions with **TPP**.

Identification of products and intermediates. Confirmation that hydroxylamine acts as an oxygen nucleophile comes from product studies. The initial product (**1**, Scheme 3) is not stable, but can be trapped. We showed previously that hydrazine is produced, together with N_2 , in the dephosphorylation of a simple triester;²¹ and explained how this is evidence for oxygen attack on P. We have used the same technique to show that hydrazine is produced in the reaction of NH_2OH with **TPP**. (i) On adding the reaction mixture to a solution of 4-(dimethylamino)benzaldehyde we observe a peak in the visible spectrum (λ_{max} 454 nm, Figure

S.6 in the Supporting Information) consistent with the formation of the hydrazone (for details see the experimental section). We presume that hydrazine is formed as shown in Scheme 4:

View Article Online
DOI: 10.1039/C3OB40988K

where the O-phosphorylated hydroxylamine intermediate (**1**), formed by nucleophilic oxygen attack by hydroxylamine on the phosphorus atom of **TPP**, reacts with neutral hydroxylamine (present in excess in the solution) to form diimide: which rapidly disproportionates to form hydrazine and nitrogen. Note that the initial product **1** from the reaction of the triester has a very good (diaryl phosphate anion, $pK_a < 2$) leaving group attached to the hydroxylamine N.



Scheme 4. Reaction of **1** with hydroxylamine, and formation of diimide and hydrazine.

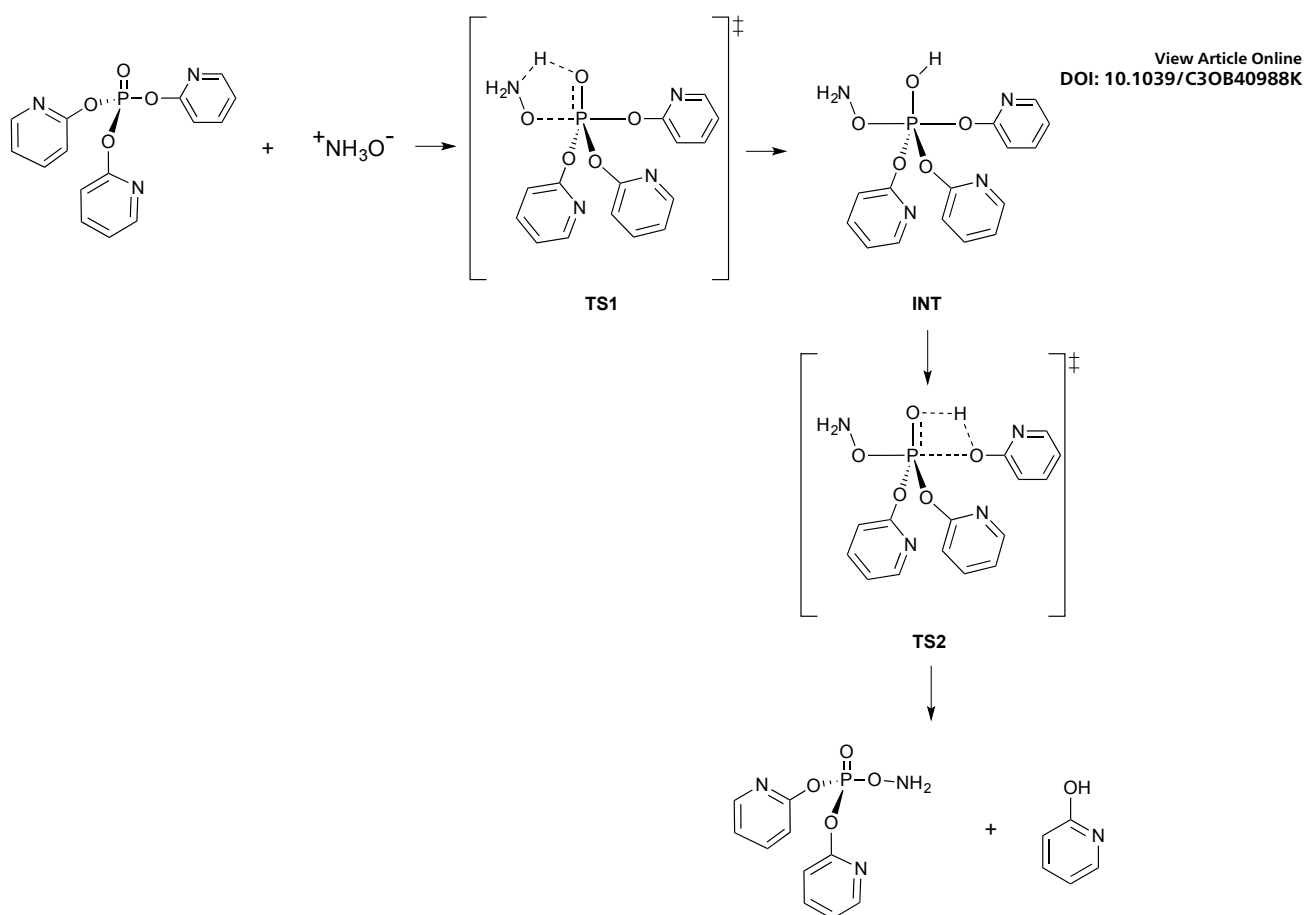
To test specifically for the powerful reducing potential of diimide, we followed the reaction by ^1H NMR in the presence of added fumaric acid. The sequence of ^1H NMR spectra presented in Figure S.4 (Supporting Information) show that the fumaric acid present is indeed reduced quantitatively to succinic acid, consistent with it trapping the strongly reducing diimide $\text{HN}=\text{NH}$. And now the reaction solution shows no significant absorbance at 454 nm, confirming that hydrazine is no longer formed (Supporting Information, Figure S.6). The reaction was also followed by ^{31}P NMR which shows, consistent with the corresponding ^1H NMR sequence (Figures S.4 and S.5 in the Supporting Information), that the intermediates shown in Scheme 4 are too unstable to be observed directly by conventional spectroscopic methods. Relevant ^1H and ^{31}P NMR chemical shifts are presented in the experimental section (Table 6). The NMR results are fully consistent with attack by hydroxylamine oxygen on ester P.

Theoretical calculations and mechanism. We have suggested a plausible reaction mechanism (Scheme 3) to explain the observed reaction of **TPP** with hydroxylamine, involving general base catalysis of the initial step. This is consistent, but not uniquely consistent, with the experimental evidence. Apparently simple phosphoryl transfer reactions can be relatively complex: even the spontaneous hydrolysis reaction involves several water molecules in the formation and/or stabilization of the transition state.²² So we performed theoretical calculations to investigate the detailed mechanism of the reaction of neutral **TPP** with hydroxylamine leading to 2-pyridone and the phosphorylated hydroxylamine.

View Article Online
DOI: 10.1039/C3OB40988K

We use Density Functional Theory (DFT) with the hybrid functional B3LYP and 6-31++G(d,p) basis set, evaluating the Potential Energy Surface (PES) in order to locate stationary points for reactants (**R**), transition states (**TS**) and products (**P**); and frequency calculation to obtain activation parameters. Since solvent undoubtedly influences structure geometries, the calculations were performed in the implicit presence of water as solvent, using the polarizable continuum model (PCM) and solvation model density (SMD). Additional, explicit water molecules were used in the calculations to allow for specific proton transfer and hydrogen bonding interactions.

As found previously for the hydrolysis reaction of **TPP**,¹⁸ all calculational attempts to find concerted displacement mechanisms led to the formation of pentacoordinate intermediates. We therefore consider mechanisms involving initial attack of the zwitterion $^+\text{NH}_3\text{—O}^-$ on the phosphorus centre of **TPP** to form a pentacoordinate addition intermediate (**Int**), which is converted to the final product by the departure of the 2-pyridyl leaving group (Scheme 5). A few added water molecules play specific roles, as catalytic general bases or for hydrogen bonding stabilisation. Table 4 compares calculated and experimentally observed activation free energies for the reaction first order in hydroxylamine (Mechanism 1, Figure 4).



Scheme 5. Mechanism 1: The basic addition-elimination mechanism (no discrete waters added) for the attack of ammonia oxide.

The results (Table 3) show good agreement between theoretical results and experiment for Mechanism 1, best when two or three additional water molecules assist the reaction by supporting two undemanding proton transfers, via a concerted cyclic activated complex which delivers an element of intramolecular general base catalysis. A major decrease, from 2.386 Å to 1.688 Å, in the interatomic distance H₅-O₆ is observed on going from INT to TS2. The length of the P₁-O₆ bond to the leaving group increases significantly from intermediate to transition state, from 1.754 Å to 2.281 Å, respectively. The dihedral angles (Table S.7 in the supporting information) indicate (in all cases) a non-planar six-membered cyclic activated complex P₁-O₂-H₃-O₄-H₅-O₆, with imaginary frequencies of 193.1. These correspond to the rocking vibration

leading to product formation. The displacement vectors (DV) associated with the imaginary frequency are indicated in Figure 5.

View Article Online
DOI: 10.1039/C3OB40988K

Adding more than three water molecules changes the calculated free energy of activation hardly at all, so that three discrete water molecules appear sufficient to describe the process in detail. The positioning of the solvent molecules and their specific roles are similar to those reported in the literature for the hydrolysis reactions of phosphate triesters.¹⁸ Figure 5 shows optimized transition state structures for the formation (TS1) and cleavage (TS2) of the pentacoordinate intermediate formed in Mechanism 1; with three water molecules playing well-defined roles in its formation and cleavage. (Cartesian coordinates for all structures appear in the Supporting Information.)

Table 3. Activation free energies, ΔG^\ddagger (kcal/mol), for the addition-elimination reaction between TPP and hydroxylamine at 25 °C, calculated at the B3LYP/6-31++g(d,p) level of theory using the PCM solvation model.

Mechanism 1: first order in hydroxylamine		Mechanism 2: Second order in hydroxylamine	
0 H ₂ O	25.3	0 H ₂ O	21.5 (21.1) ^a
1 H ₂ O	22.6	1 H ₂ O	24.0
2 H ₂ O	21.2	Obs. (expt.)	19.1 ^b
3 H ₂ O	20.2		
4 H ₂ O	20.5		
Obs. (expt.)	20.7 ^b		

^a Value obtained for TS5. ^b Corrected (by -1.0 kcal/mol) for the 18% of reactive ⁺NH₃-O⁻ present.

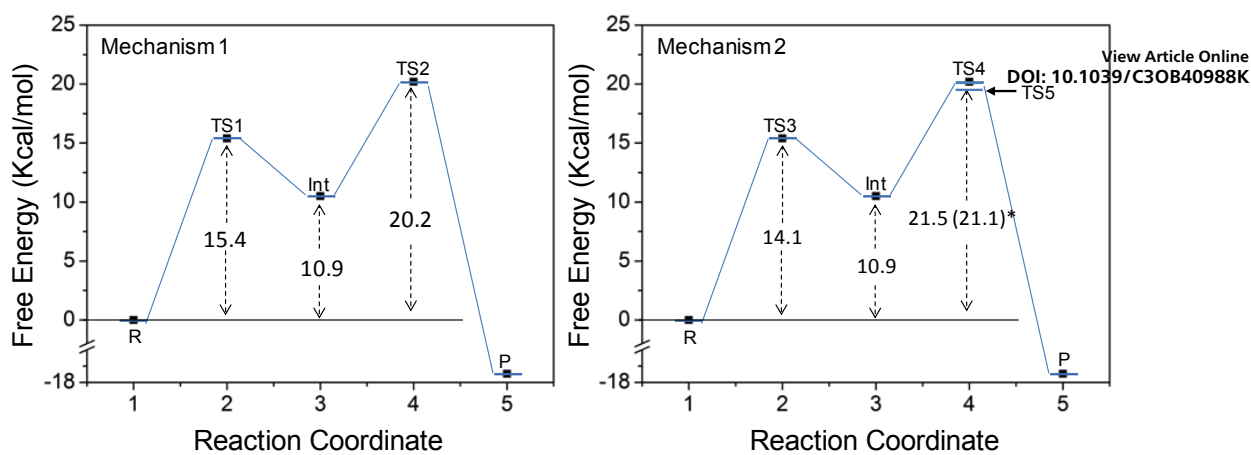


Figure 4. Free energy profiles for Mechanisms 1 and 2 respectively). The lifetimes of the intermediates are predicted to be minimal.

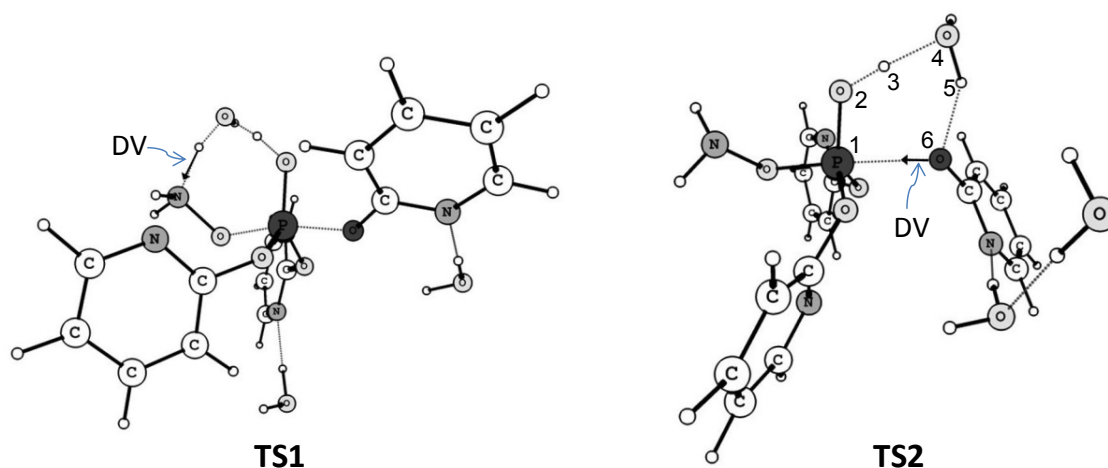
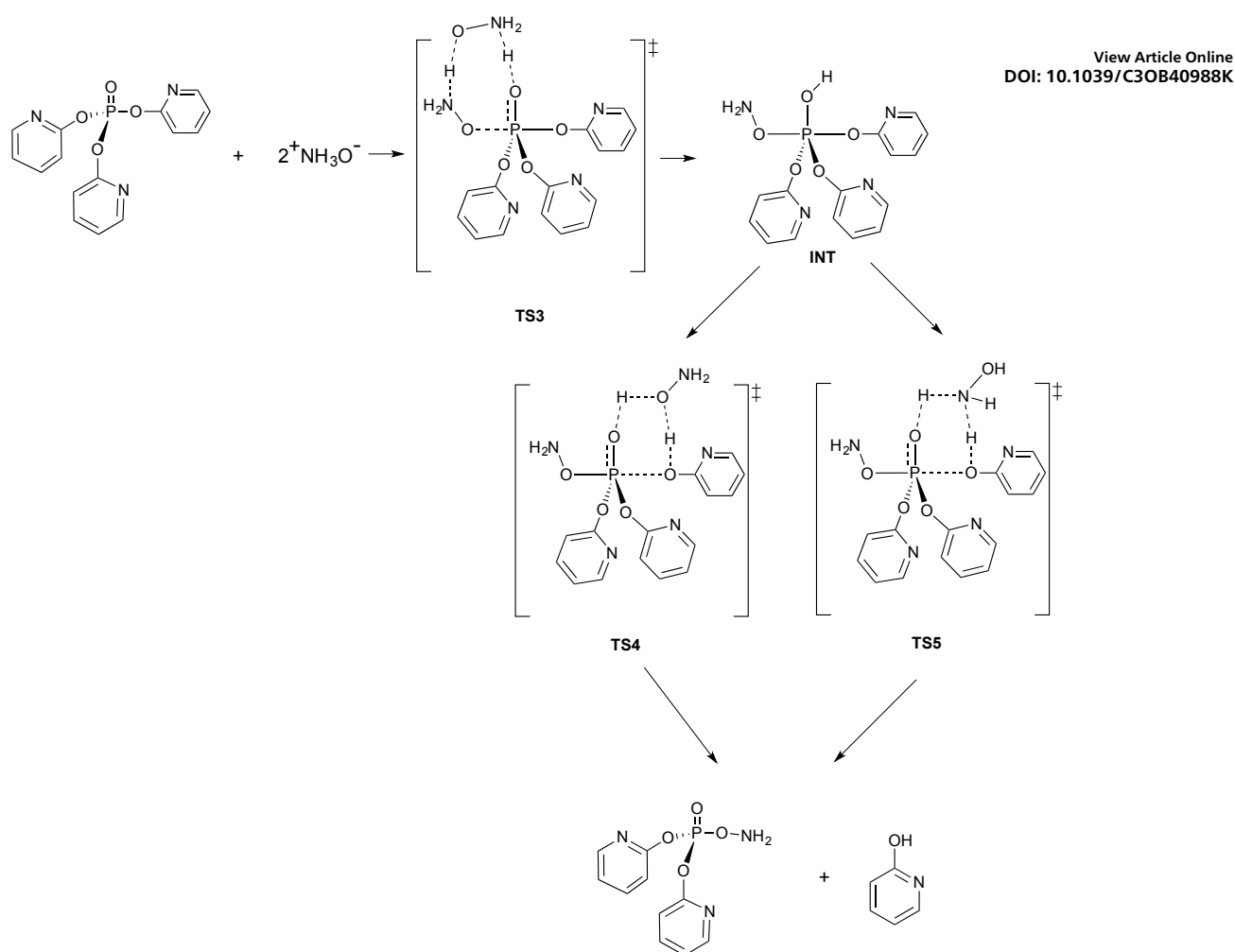


Figure 5. Optimized structures for TS1 and TS2 for Mechanism 1, the reaction first order in hydroxylamine: in the presence of 3 discrete water molecules (see the text).

As shown by the energy-profile diagrams of Figure 4, the significant conclusion from the calculations is that the second step, the cleavage of the pentacoordinate addition intermediate, is rate-determining. Thus the observed general base catalysis of the reaction with hydroxylamine must be of the second step of the reaction. We therefore carried out similar calculations for

Mechanism **2** (Scheme 6), to include a second molecule of hydroxylamine. The results suggest that the driving force for the cleavage of the neutral intermediate develops from the removal of the proton from the P—O(2)H bond by the general base: which initiates a loosely concerted cyclic process leading eventually to the transfer of a proton to the leaving group with cleavage of P—O(6) (Schemes 4 and 6). The general base is water in **TS2**, the OH group of NH₂OH in **TS4**, and – most effective – the NH₂ group in **TS5**. The OH groups of water and NH₂OH support closely similar pathways: the NH₂ group has the advantage of being more basic, so that the initial proton transfer is already complete in **TS5**, generating HONH₃⁺ as a general acid with one of its N⁺H protons in position to assist the departure of the leaving group. We note that the addition of discrete water molecules to the calculation does not improve the agreement with experiment when two hydroxylamines are present (Table 3). The second, catalytic, hydroxylamine takes the place of discrete waters, in a PCM environment specifically parameterised for water.

View Article Online
DOI: 10.1039/C3OB40988K



Scheme 6. Mechanism 2. The addition-elimination mechanism involving two (zwitterionic) hydroxylamines. The formation of the intermediate, via **TS3**, involves general base catalysis, much as suggested in Scheme 3, but this step is rapidly reversible before the rate determining breakdown of the intermediate. The pathway via **TS5** is (modestly) preferred (Table 4).

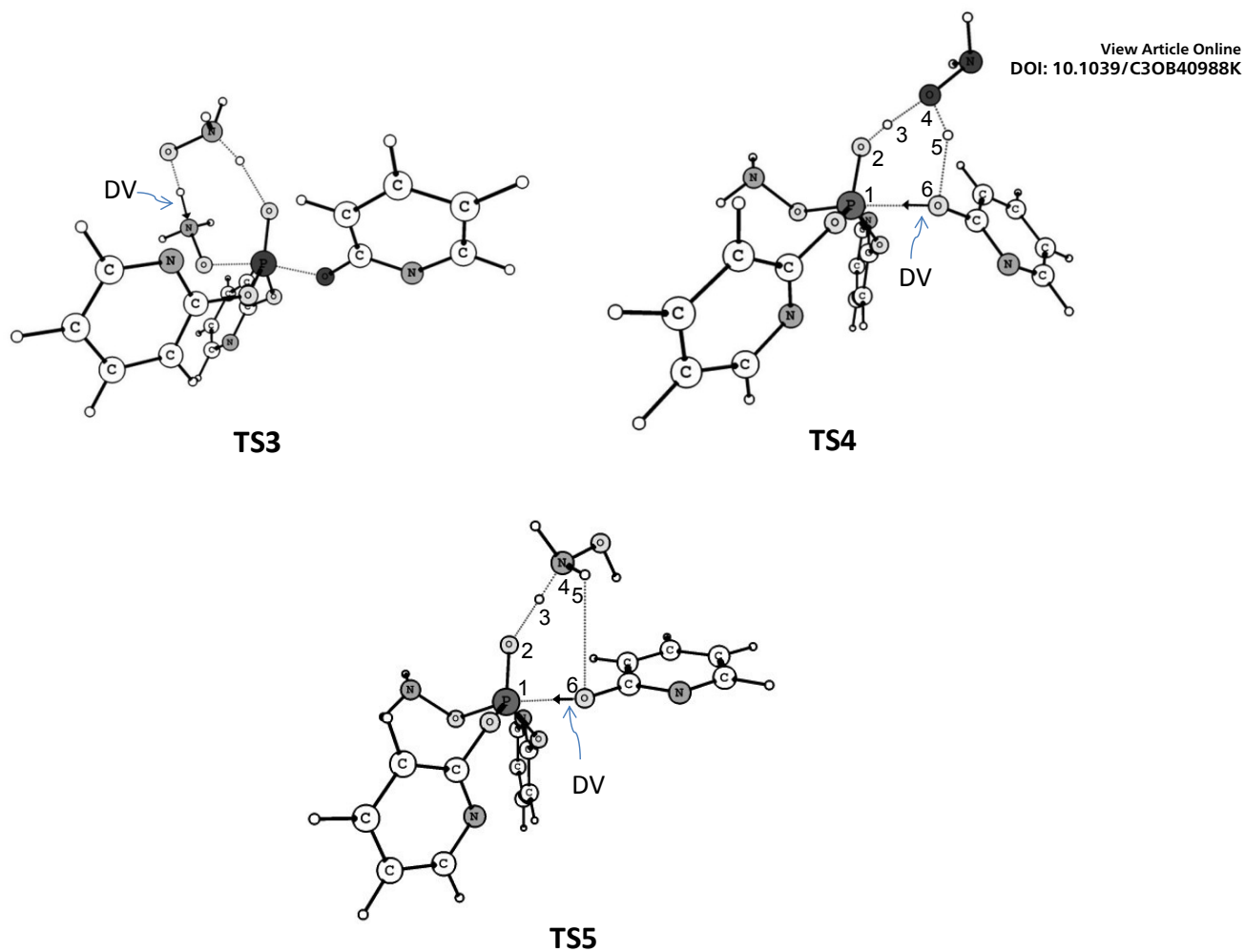
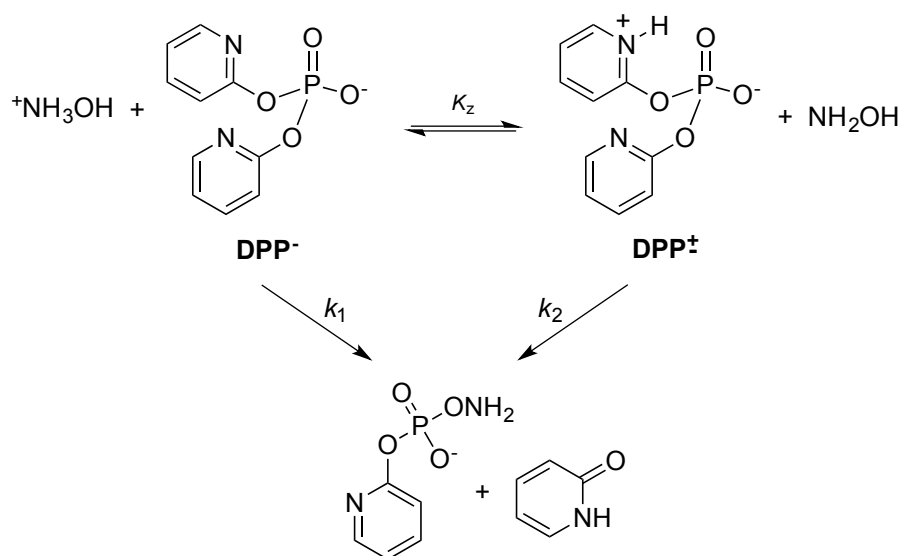


Figure 6. Optimized structures for TS3, 4 and 5 of Mechanism 2, the reaction second order in hydroxylamine (Scheme 6). The second molecule of NH_2OH acts more or less directly as a general acid in the second, breakdown step (TS5).

Reaction of DPP with hydroxylamine

View Article Online
DOI: 10.1039/C3OB40988K

Kinetics. Reactions were performed as for **TPP**, in aqueous media and under pseudo-first order conditions with respect to the substrate, by monitoring the appearance of product 2-pyridone at 294 nm. Figure 1 (above) compares the pH-rate profile for the reaction of **DPP** with 1M hydroxylamine with that for its spontaneous hydrolysis, and shows that k_{obs} for the reaction with hydroxylamine falls as the pH increases from pH 5 to 9, behavior different from that observed in our previous studies of reactions of phosphate esters with hydroxylamine.^{16, 23} The fractional composition profiles for substrate and nucleophile, shown in Figure S.7 of the Supporting Information, show that over this pH range the substrate is present almost exclusively as the **DPP**⁻ anion. ⁺NH₃OH ($pK_a = 6.06$) is not a nucleophile, so the pH-dependence indicates that the observed reaction must involve the kinetically equivalent reaction of hydroxylamine with the **DPP**[±] zwitterion. This is confirmed by the solvent kinetic isotope effect, measured as 0.64 in D₂O at pD 5.0 and 25°C. The inverse isotope effect is consistent with a (formal) preliminary proton-transfer equilibrium between the weakly reactive **DPP**⁻ and the non-reactive ⁺NH₃OH (Scheme 7).



Scheme 7. Reactions of **DPP**[±] and **DPP**⁻ with hydroxylamine.

The pH-rate profile was fitted to equation 3, which describes the reaction of hydroxylamine with **DPP**[±] (k_2) (Scheme 7). Eq. 3 also includes a term for the hydrolysis of **DPP**[±] (k_{\pm}), which makes a small contribution to k_{obs} at lower pHs (the initial hydrolysis products are 2-pyridone and 2-pyridyl phosphate).

$$k_{\text{obs}} = (k_2 \cdot \chi_{\text{NH}_2\text{OH}} \cdot \chi_{\text{DPP}^{\pm}}) + k_{\pm} \cdot \chi_{\text{DPP}^{\pm}} \quad (3)$$

χ_{DPP^-} , $\chi_{\text{DPP}^{\pm}}$, $\chi_{\text{NH}_2\text{OH}}$ and $\chi_{\text{NH}_3^+\text{OH}}$ are the molar fractions of **DPP**⁻, **DPP**[±], **NH**₂**OH** and ⁺**NH**₃**OH**, respectively.

The kinetic parameters obtained from the fit to eq. 3 (Table 4) show that the dephosphorylation of **DPP**[±] by 1M neutral hydroxylamine (k_2) is enhanced about 1200-fold), compared to the spontaneous hydrolysis reaction. Any contribution to k_{obs} of the reaction of **NH**₂**OH** with **DPP**⁻ is minimal, consistent with the poor leaving group. In contrast to the behavior observed for the reaction of hydroxylamine with **TPP**, k_{obs} for the reaction with **DPP** shows a simple linear dependence on nucleophile concentration (the data are shown in Table S.5 of the Supporting Information).

Table 4. Kinetic parameters for the reaction of **DPP** with hydroxylamine, at 25°C.^{a,b}

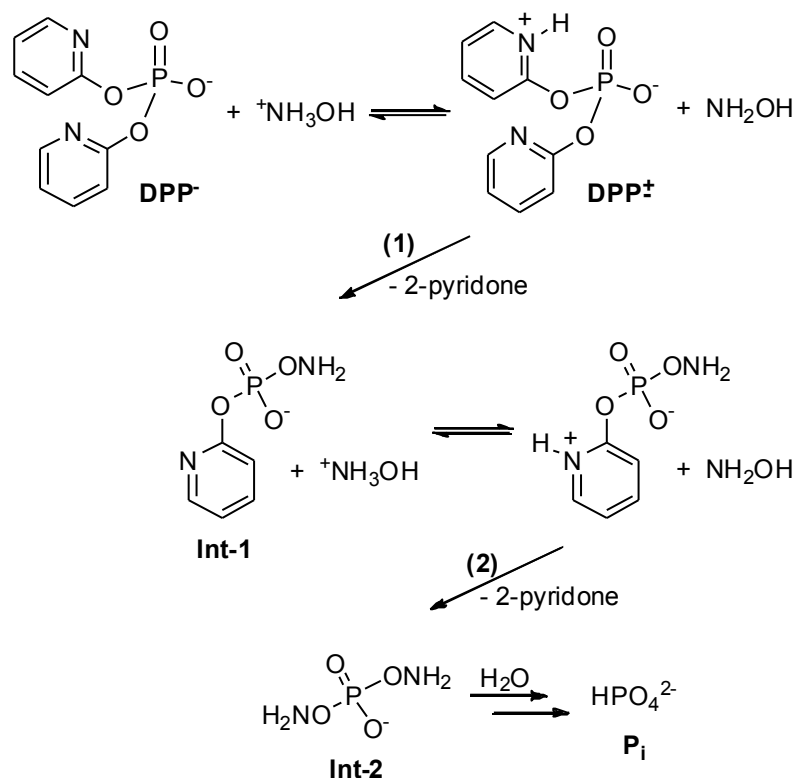
$k_{\pm}, \text{s}^{-1} \text{ }^c$	3.56×10^{-4}
$k_1, \text{M}^{-1} \text{s}^{-1}$	2.26×10^{-4}
$k_2, \text{M}^{-1} \text{s}^{-1}$	4.22×10^{-1}
$\text{p}K_{\text{a}} (\text{}^+\text{NH}_3\text{OH}) \text{ }^c$	6.06
$\text{p}K_{\text{a}} (\text{DPP}^{\pm}) \text{ }^c$	2.73

^a Obtained by fitting the pH-rate profile (Figure 1) to eqs. 3. ^b Rate constant for **DPP**⁻ hydrolysis: $3.12 \times 10^{-10} \text{ s}^{-1}$.¹¹ ^c Literature values.^{11,24}

Identification of products and intermediates. We followed the reaction of **DPP** with hydroxylamine by ^1H and ^{31}P NMR, and performed mass spectroscopic analysis (ESI-MS and the tandem version, ESI-MS/MS) to confirm the identities of products and intermediates.

View Article Online
DOI: 10.1039/C3OB40988K

NMR experiments were performed at pD 5, in the plateau region of the pH-rate profile (Figure 1), where the predominant reaction is that of the **DPP**[±] zwitterion with neutral hydroxylamine. Chemical shifts for all the species detected are presented in Table 6 (below). Sequential ^1H NMR spectra (Figure S.8 in the Supporting Information) show the disappearance of the substrate **DPP** together with the formation of 2-pyridone as the sole final product, consistent with exclusive attack of hydroxylamine oxygen on the phosphorus atom of **DPP**. The ^1H NMR spectra also reveal the formation and disappearance of a phosphorylated intermediate, stable enough to be observed directly by conventional NMR techniques and consistent with structure **Int-1** in Scheme 8.



Scheme 8. Equilibria involved in the consecutive reactions of **DPP** with hydroxylamine, in buffered aqueous solution.

Successive ^{31}P NMR spectra (Figure S.9, Supporting Information) also show the appearance of a peak at -1.46 ppm consistent with **Int-1** formation in addition to the disappearance of **DPP**. The subsequent disappearance of the -1.46 ppm peak is accompanied by the appearance of a new peak at 8.16 ppm, suggesting that **Int-1** is not hydrolyzed but itself reacts (much faster, as would be expected) with hydroxylamine. The pyridine N of **Int-1** (Scheme 8) will be at least as basic as that of **DPP**⁻, and attack by hydroxylamine on the zwitterion (reaction 2) to form **Int-2** is expected to be its dominant reaction.

We observed similar behaviour in previous studies of the nucleophilic reaction of imidazole with a phosphate diester with two 2,4-dinitrophenyl groups.⁹ In that case also both good (2,4-dinitrophenolate) leaving groups were displaced in successive steps by nucleophilic attack of imidazole on phosphorus, to produce a bis-phosphorylimidazole intermediate. Which finally decomposed to inorganic phosphate in two steps with regeneration of imidazole. It appears that **Int-2** is similarly, though more slowly, hydrolyzed, to regenerate hydroxylamine and form inorganic phosphate, **P_i** (0.85 ppm). The small amounts of **P_i** observed before the decomposition of the intermediates, are presumably a small contribution from the spontaneous hydrolysis of **DPP**[±]. The mechanism summarized in Scheme 8 explains why we observe (spectrophotometrically) the release of both 2-pyridone groups of **DPP**, but observe no monoester **MPP** in either ^1H or ^{31}P NMR experiments.

Building on our experience of studying mechanisms using mass spectrometric techniques, we performed ESI-MS analysis to monitor the reaction of **DPP** with hydroxylamine: the results add further support for the formation of **Int-1** (Scheme 8). As described above, in the ESI-MS process used here, solvated ions are “fished and transferred” directly from solution to the gas phase, so that the experiments provide “snapshots” of the ions present in solution. These have been shown in numerous cases to reflect accurately the actual ionic composition.^{9, 25, 26}

Samples of reaction solution at pH 5.0 and 25 °C, containing all reactants, intermediates, and products, were transferred directly to the gas phase and detected by ESI(+)-MS. Initially, ESI-MS(+) showed a series of major species in solution (Figure 7), indicating the presence of 2-hydroxypyridine (the protonated species at m/z 96) as the major product, and a species of m/z 191, consistent with (the protonated form) of **Int-1** of Scheme 11,

View Article Online
DOI: 10.1039/C3OB40988K

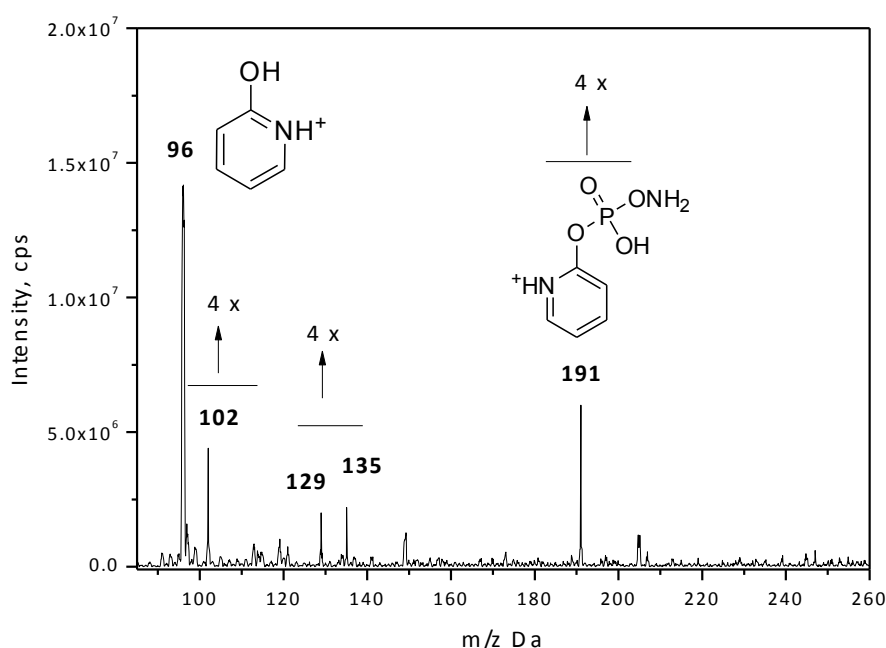


Figure 7. ESI(+)-MS of the reaction of **DPP** (Li^+ salt) with 1M hydroxylamine, after 180 minutes of reaction, at pH 5 and 25°C. Suggested assignments for minor peaks (intensities magnified 4x) are: 102 = pyridone + Li; 129 = **Int-2**; 135 = **Int-2** + Li.

Theoretical calculations. To further clarify the mechanism of the reaction of **DPP** with hydroxylamine, leading to **Int-1** and 2-pyridone, we performed theoretical calculations, similar to those discussed above for the corresponding reaction of the triester **TPP**. We use Density Functional Theory (DFT) at the B3LYP/6-31++G(d,p) level, evaluate Potential Energy Surfaces

(PES) in order to locate stationary points for reactants (R), transition state (TS) and products (P), and use frequency calculation to obtain the activation parameters. All calculations were performed using the polarizable continuum model (PCM) and the solvation model density (SMD); and discrete water molecules were included to investigate particular proton transfers or hydrogen bonds.

View Article Online
DOI: 10.1039/C3OB40988K

The calculations refer to the initial P—O cleavage step, reaction (1) of Scheme 8. We derived Gibbs free energies of activation (ΔG^\ddagger) for three different combinations of reagents and solvent: (i) substrate and nucleophile only; (ii) substrate and nucleophile, plus one water and (iii) substrate and nucleophile plus two water molecules. Values of ΔG^\ddagger were calculated with respect to the global minimum (**R1** in Scheme 9), defined by **DPP**⁻ and H₃N⁺OH. Consistent with the consensus that the hydrolysis reactions of phosphate diesters with good leaving groups do not involve pentacovalent phosphorane dianion intermediates, we found previously that all attempts to optimize the structure of a pentacoordinate intermediate in the hydrolysis of **DPP** led to cleavage of the P—O_{LG} bond and reversion to the bimolecular, S_N2(P) transition state.¹¹ We therefore consider only concerted mechanisms for the reaction with hydroxylamine.

The results (Table 5) show a calculated ΔG^\ddagger in good agreement with the experimental data when one water molecule is taken into account in the TS structure. This water molecule provides a TS stabilization of about 2 kcal/mol, compared with the reaction in the absence of a discrete water: including a second water molecule provides no additional stabilization. The calculation therefore focused on the S_N2(P) mechanism **B** of Scheme 9, involving oxygen attack on phosphorus, with the single water molecule hydrogen-bonded to both nucleophile and phosphoryl group as shown. We present a full characterization of the transition state for this mechanism, and a detailed description of the changes in geometrical parameters, charges and Wiberg indexes. Note that the immediate nucleophile considered in the calculations is the

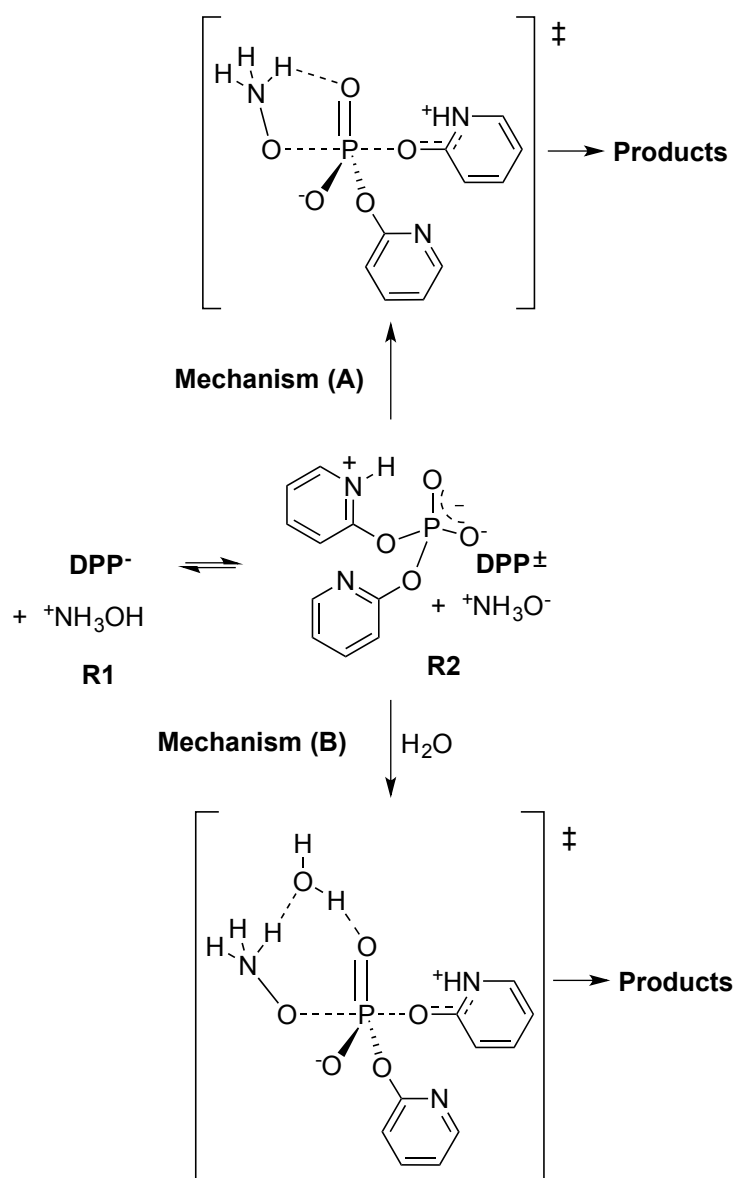
zwitterionic ammonia oxide, which we have shown makes up some 20% of hydroxylamine in aqueous solution.¹⁷

View Article Online
DOI: 10.1039/C3OB40988K

Table 5. Free energies of activation and second order rate constants for the reaction of hydroxylamine with di-2-pyridyl phosphate at 25 °C, calculated at the B3LYP/6-31++G(d,p) level of theory.

Number of water molecules	k ($M^{-1} s^{-1}$)	ΔG^\ddagger (kcal/mol)
0	0.006	20.5
1	0.22	18.3
2	0.23	18.3
Experimental ^a	0.42	18.0

^a Experimental ΔG^\ddagger obtained from second order rate constant (**Table 4**).



Scheme 9. Two possible mechanisms for the reaction of **DPP** with hydroxylamine. Mechanism **B** considers one added water molecule. The (initial) products are the phosphorylated hydroxylamine (**Int-1** in Scheme 8) and 2-pyridone.

View Article Online
DOI: 10.1039/C3OB40988K

Figure 8 presents the optimized TS structure for Mechanism **B**, and the atom numbering used: and shows the formation of the new P₂-O₃ bond (involving the attack of the ammonia oxide oxygen on phosphorus) and the cleavage of the P₂-O₁ bond. Cartesian coordinates for the reactants, transition state and products are given in the Supporting Information, and structural parameters of reactants, transition state, and product of the rate-determining step are given in Table S.9. The interatomic distances show an important elongation of the P₂-O₁-bond to the leaving group, from 1.693 Å in the reactants to 1.840 Å in the TS, indicating significant bond breaking. This accompanies the formation of O₃-P₂, the non-bonded 5.917 Å shortening to 2.234 Å. The bond distances N₄-H₅ and O₉-H₁₀ do not change significantly from reactant to TS, indicating that the stabilization promoted by the water molecule only involves hydrogen bonding.

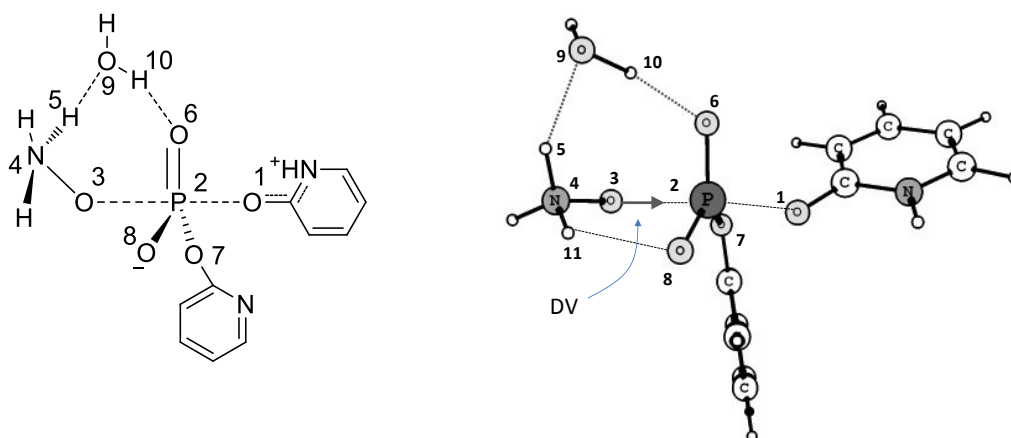


Figure 8. Transition state (TS) for mechanism **B** of Scheme 9. The transition DV is associated with a rocking vibration leading to product formation.

Figure 9 shows the calculated free energy profile for this reaction. The optimized TS of the rate-determining step connects reactants and products in a single step, concerted $S_N2(P)$ mechanism.

View Article Online
DOI: 10.1039/C3OB40988K

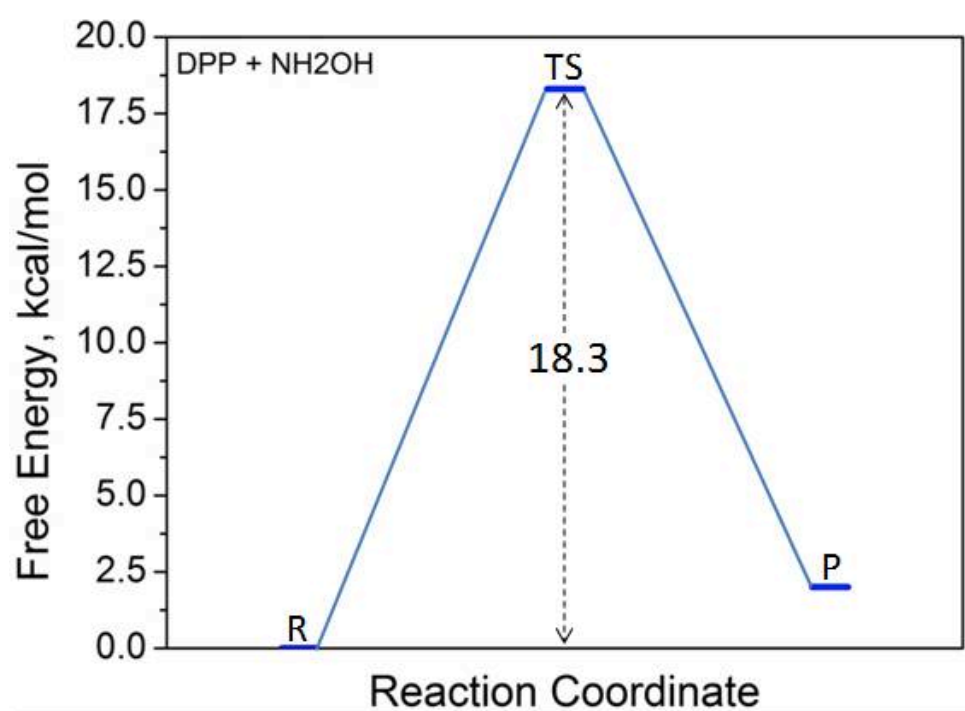


Figure 9. Free energy profile for the nucleophilic attack of hydroxylamine on DPP^- .

Conclusions

The 400-fold enhancement of reactivity of the α -nucleophile hydroxylamine towards the triester **TPP** is far greater than towards the DPP^- anion: consistent with previous results with simple phosphate esters, which showed rate enhancements for the reactions with triesters > diester anions > monoester dianions.¹⁶ The second (rate-determining) step of the addition-elimination reaction with the triester **TPP** produces an O-phosphorylated hydroxylamine with a very good leaving group attached to N: this intermediate rapidly decomposes with N—O cleavage, forming dimide. By contrast, the $ArOP(O_2)-ONH_2$ product of the (concerted) $S_N2(P)$ reaction with the DPP^- anion reacts a second time with NH_2OH to form $(NH_2O)_2PO_2^-$, which is subsequently hydrolysed with P— ONH_2 cleavage to inorganic phosphate.

The PCM solvation model has a generally poor reputation for describing interactions between water molecules and reactants, especially in hydrolysis reactions, where proton transfers and hydrogen bond formation and cleavage take place. Our results from this and recent work show that the explicit inclusion of water molecules playing specific roles is a key to calculating convincing model transition states for this type of reaction. The specific roles imply specific geometrical arrangements, which are based on our experience of organic reaction mechanisms.

View Article Online
DOI: 10.1039/C3OB40988K

Experimental section

Materials. The phosphate esters **TPP** and **DPP** were prepared as described previously.^{11, 15, 27} Inorganic salts were of the best analytical grade available from commercial sources (Merck, Aldrich, Fluka and Across Organics) and were used as received. Liquid reagents were purified by distillation.

Kinetics. Reactions of **TPP** and **DPP** with hydroxylamine were followed spectrophotometrically by monitoring the appearance of 2-pyridone at 294nm. Reactions were started by adding 30 μ L of 5mM stock solutions of the substrate to 3 mL of buffered aqueous solutions to give final substrate concentrations of 50 μ M. Hydroxylamine concentrations were in great excess to guarantee pseudo-first order kinetics with respect to the substrate. The temperatures of the reaction solutions in quartz cuvettes were controlled with a thermostatted water-jacketed cell holder, and ionic strengths were maintained ($I=1.0$) with KCl. The pH was maintained with 0.01M buffers of CH₃COOH, NaH₂PO₄, BISTRIS and TRIS. Absorbance versus time data were stored directly on a microcomputer, and observed first-order rate constants, k_{obs} , were calculated using absorbance changes obtained for at least 90% of the reaction, using an iterative least-squares program; correlation coefficients were > 0.999 for all kinetic runs. For the solvent deuterium isotope effect measurement, the comparison was made at

0.5M hydroxylamine, at pD(pH) 8.5 (conditions as for the second order plot of Figure 2). Under these conditions the hydroxylamine is present exclusively as the free base, and the third order process represents 94% of the total reaction. The pD was obtained from the meter reading using the relation $pD = pH + 0.4$ at 25°C.²⁸

View Article Online
DOI: 10.1039/C3OB40988K

Hydrazine trapping. The procedure adopted, taken from Watt and Chrisp,²⁹ is briefly described as follows: 50μL of a 0.01M solution of substrate **TPP** in acetonitrile were added to 1mL of a 0.05M hydroxylamine solution buffered at pH 8.50 with 0.01M TRIS. After stirring for 1h at 25°C, an aliquot of 100μL of the reaction mixture was added to 2mL of a freshly prepared color reagent. The product, *p*-dimethylaminobenzaldehyde hydrazone, was identified by UV-Vis spectroscopy (λ_{max} 454nm, ϵ 59000)³⁰ recorded using a HP8453 spectrophotometer. A control experiment, using a solution prepared by the above procedure but without the triester, gave no significant absorbance at 454nm.

Diimide trapping. For diimide trapping, it was prepared a mixture in D₂O by adding 50μL of a 0.01M solution of **TPP** in acetonitrile to 1mL of a 0.05M hydroxylamine solution buffered at pD 7.20 with 0.01M TRIS containing also 0.2M of fumaric acid. The reaction was followed by ¹H NMR, which showed consumption of fumaric acid and formation of succinic acid, indicating reduction by diimide. After, hydrazine trapping was tested (see experimental details and conditions above), but the UV-Vis spectrum showed no significant absorbance at 454nm, confirming effective diimide trapping.

Following reactions by NMR. We followed the reactions of **TPP** and **DPP** with hydroxylamine in D₂O at 25°C, using both ¹H and ³¹P NMR. Reactions of **TPP** with NH₂OH were performed at pD 7.2, and reactions of **DPP** with the nucleophile, at pD 5.0. Hydroxylamine concentration was in large excess in respect to that of the substrate. ¹H NMR spectra were monitored on 400 or 200MHz spectrometers and chemical shifts are referred to internal sodium 3-(trimethylsilyl) propionate (TMSP) as standard. ³¹P NMR experiments were performed on a 200MHz

spectrometer using phosphoric acid (85%) as external reference, using 50 mM **DPP** and 20 mM

View Article Online
DOI: 10.1039/C3OB40988K

TPP. ^1H and ^{31}P NMR chemical shift assignments are presented in Table 6.

Table 6. ^1H and ^{31}P NMR chemical shifts of the species observed in the reactions of **TPP** and **DPP** with hydroxylamine, in D_2O , at 25°C .^{a-c}

Species	^1H NMR, δ (ppm)	^{31}P NMR, δ (ppm)
TPP	7.14 ppm (dd, 1H, J= 7.4, 5.4 Hz); 7.29 ppm (dd, 1H, J= 8.2, 0.8 Hz); 7.88 ppm (ddd, 1H, J= 8.2, 7.4, 2.0 Hz); 8.13 ppm (ddd, 1H, J= 5.4, 2.0, 0.8 Hz)	-19.63
DPP	7.13 ppm (ddd, 1H, J= 8.2, 2.0, 0.8 Hz); 7.19 ppm (ddd, 1H, J= 7.4, 5.1, 0.8 Hz); 7.80 ppm (ddd, 1H, J= 8.2, 8.2, 2.0 Hz); 8.12 ppm (dd, 1H, J= 5.01, 2.0 Hz)	-11.58
Int-1 (reaction of DPP with NH_2OH)		-1.46
Int-2 (reaction of DPP with NH_2OH)		8.16
P_i		0.85
2- pyridone	6.51 ppm (ddd, 1H, J= 7.2, 6.6, 1.2 Hz); 6.66 ppm (ddd, 1H, J= 9.2, 1.1, 1.1 Hz); 7.44 ppm (ddd, 1H, J= 6.6, 2.0, 0.8 Hz); 7.62 ppm (ddd, 1H, J= 9.4, 7.4, 2.3 Hz)	—
Succinic acid	2.40 (s, 4H)	—
Fumaric acid	6.53 (s, 2H)	—

^a Chemical shifts for the phosphate esters, 2-pyridone, succinic and fumaric acid and P_i are consistent with values obtained from spectra of the pure compounds and/or from the literature.¹⁵

²¹ ^b Structures for **Int-1** and **Int-2** are presented in Scheme 8. Assignments of ^{31}P NMR are consistent with chemical structure, but assignment of ^1H NMR are less secure since some peaks overlap with those of **DPP**. ^c In the reaction of **DPP** with hydroxylamine, we identified three minor peaks in the ^{31}P NMR, but could not make positive structural assignments. Nevertheless their observed low intensities are consistent with Scheme 8 as a major path for the dephosphorylation of **DPP**.

We do not have direct evidence from the ^{31}P NMR data for hydroxylamine regeneration in the reaction with **DPP**, because the pH of the reaction medium changes considerably with the continuing generation of P_i . This makes difficult secure assignment of the peaks from the spectrum after 350 min, and specifically the identification of the species formed from the

decomposition of **Int-2**. The results are consistent with the considerable stability of the intermediates **Int-1** and **Int-2**.

View Article Online
DOI: 10.1039/C3OB40988K

Mass Spectrometry. In order to identify intermediates and reaction products, direct infusion electrospray ionization mass spectrometry analyses were performed with a hybrid triple quadrupole linear ion-trap mass spectrometer. For typical electrospray ionization (ESI-MS) conditions, **DPP** was reacted with NH_2OH (1M) in an aqueous medium at pH 5. A microsyringe pump delivered the reagent solution into the ESI source at a flow rate of $10 \mu\text{L min}^{-1}$. ESI and the QqQ (linear trap) mass spectrometer was operated in the positive-ion mode. Main conditions: curtain gas nitrogen flow of 20 mL min^{-1} ; ion spray voltage of -4500 eV ; declustering potential of -21 eV ; entrance potential of -10 eV ; and collision cell exit potential of -12 eV .

Theoretical calculations. Quantum theoretical calculations for reactions of the phosphate esters with hydroxylamine were performed at the B3LYP level of theory, with basis set 6-31G++(d,p) and 6-31G+(d,p) for reactions of **TPP** and **DPP**, respectively, using the GAUSSIAN 09 package implemented in Linux operative systems.³¹ The default parameters for convergence were used, i.e, the Berny analytical gradient optimization routine, convergence on the density matrix was 10^{-9} atomic units, threshold value for maximum displacement 0.0018 \AA , and maximum force $0.00045 \text{ Hartree/Bohr}$. The structures corresponding to the energy minima and the transition state were characterized by frequency calculations at 1 atm and 298.15 K .³² The transition state (TS) was obtained by the Quadratic Synchronous Transit (QST) protocol.

Solvent effects are important, not least for hydrolysis processes, and can affect structure geometries significantly. We performed substrate optimizations using SCRF keyword and the Polarizable Continuum Model (PCM) and the SMD solvation model.^{33, 34} The applicability of the implicit solvation model has been questioned, in the context of a mechanistic study of

phosphate diester hydrolysis.³⁵ The appropriate model for a particular reaction must of course always be chosen with due care. But for calculations involving water as a reactant the combination of implicit and explicit solvation methodologies is both practical and appropriate: since proton transfers are an integral part of the chemistry (and an isolated water molecule is statistically insignificant).

View Article Online
DOI: 10.1039/C3OB40988K

Supporting Information. Tables, equations and figures of kinetic, ¹H and ³¹P NMR and MS data. Cartesian coordinates for reactant, transition state and product calculated at B3LYP/6-31G++(d,p) or B3LYP/6-31G+(d,p) level of theory. This material is available from

Author information

Corresponding Author:

Prof. Anthony J. Kirby, University Chemical Laboratory, Cambridge CB2 1EW, UK.

E-mail: ajk1@cam.ac.uk

Acknowledgements. We thank INCT-Catálise and the Brazilian foundations CNPq, CAPES and FAPESC for financial assistance.

References

1. A. C. Hengge, *Adv Phys Org Chem*, 2005, 40, 49-108.
2. W. W. Cleland and A. C. Hengge, *Chem Rev*, 2006, 106, 3252-3278.
3. J. K. Lassila, J. G. Zalatan and D. Herschlag, *Annu Rev Biochem*, 2011, 80, 669-702.
4. A. J. Kirby and A.G.Varvoglis, *J Am Chem Soc*, 1967, 89, 415-&.
5. A. J. Kirby and A.G.Varvoglis, *J Chem Soc B*, 1968, 135-&.
6. A. J. Kirby and M. Younas, *J Chem Soc B*, 1970, 510-513.
7. A. J. Kirby and M. Younas, *J Chem Soc B*, 1970, 1165-1172.
8. S. A. Khan and A. J. Kirby, *J Chem Soc B*, 1970, 1172-1182.
9. E. S. Orth, E. H. Wanderlind, M. Medeiros, P. S. Oliveira, B. G. Vaz, M. N. Eberlin, A. J. Kirby and F. Nome, *J Org Chem*, 2011, 76, 8003-8008.
10. M. Medeiros, E. S. Orth, A. M. Manfredi, P. Pavez, G. A. Micke, A. J. Kirby and F. Nome, *J Org Chem*, 2012, 77, 10907-10913.
11. A. J. Kirby, M. Medeiros, J. R. Mora, P. S. M. Oliveira, T. A. S. Brandão, A. Amer, N. H. Williams and F. Nome, *J. Org. Chem.*, 2013, 78, 1343-1353.

12. A. J. Kirby, M. Medeiros, P. S. M. Oliveira, E. S. Orth, T. A. S. Brandão, E. H. Wanderlind, A. Amer, N. H. Williams and F. Nome, *Chem-Eur J*, 2011, 17, 14996-15004.
13. J. Q. Liu and G. Wulff, *J Am Chem Soc*, 2008, 130, 8044-8054.
14. A. Albert and J. N. Phillips, *J Chem Soc*, 1956, 1294-1304.
15. A. J. Kirby, M. Medeiros, P. S. Oliveira, T. A. Brandão and F. Nome, *Chem-Eur J*, 2009, 15, 8475-8479.
16. A. J. Kirby, A. M. Manfredi, B. S. Souza, M. Medeiros, J. P. Priebe, T. A. S. Brandão and F. Nome, *ARKIVOC*, 2009, 28-38.
17. A. J. Kirby, J. E. Davies, D. J. Fox, D. R. W. Hodgson, A. E. Goeta, M. F. Lima, J. P. Priebe, J. A. Santaballa and F. Nome, *Chem Commun*, 2010, 46, 1302-1304.
18. J. R. Mora, A. J. Kirby and F. Nome, *J Org Chem*, 2012, 77, 7061-7070.
19. NIST Standard Reference Database 46, Version 6.0.
20. J. B. Domingos, E. Longhinotti, T. A. S. Brandão, C. A. Bunton, L. S. Santos, M. N. Eberlin and F. Nome, *J. Org. Chem.*, 2004, 69, 6024-6033.
21. A. J. Kirby, B. S. Souza, M. Medeiros, J. P. Priebe, A. M. Manfredi and F. Nome, *Chem Commun*, 2008, 4428-4429.
22. A. J. Kirby, J. R. Mora and F. Nome, *Biochim Biophys Acta*, 2012.
23. J. B. Domingos, E. Longhinotti, C. A. Bunton and F. Nome, *J Org Chem*, 2003, 68, 7051-7058.
24. M. Medeiros.
25. J. B. Domingos, E. Longhinotti, T. A. S. Brandão, C. A. Bunton, L. S. Santos, M. N. Eberlin and F. Nome, *J Org Chem*, 2004, 69, 6024-6033.
26. E. S. Orth, T. A. S. Brandão, B. S. Souza, J. R. Pliego, B. G. Vaz, M. N. Eberlin, A. J. Kirby and F. Nome, *J Am Chem Soc*, 2010, 132, 8513-8523.
27. R. S. Brown and M. Zamkanej, *Inorg Chim Acta-Bioinor*, 1985, 108, 201-207.
28. T. H. Fife and T. C. Bruice, *J Phys Chem-Us*, 1961, 65, 1079-1080.
29. G. W. Watt and J. D. Chrisp, *Anal Chem*, 1952, 24, 2006-2008.
30. G. Yagil and M. Anbar, *J Am Chem Soc*, 1962, 84, 1797-1803.
31. Gaussian 09, Frisch, M. J., G. W. Trucks, H. B. Schlegel, G. E. Scuseria, M. A. Robb, J. R. Cheeseman, G. Scalmani, V. Barone, B. Mennucci, G. A. Petersson, H. Nakatsuji, M. Caricato, X. Li, H. P. Hratchian, A. F. Izmaylov, J. Bloino, G. Zheng, J. L. Sonnenberg, M. Hada, M. Ehara, K. Toyota, R. Fukuda, J. Hasegawa, M. Ishida, T. Nakajima, Y. Honda, O. Kitao, H. Nakai, T. Vreven, J. Montgomery, J. A., J. E. Peralta, F. Ogliaro, M. Bearpark, J. J. Heyd, E. Brothers, K. N. Kudin, V. N. Staroverov, R. Kobayashi, J. Normand, K. Raghavachari, A. Rendell, J. C. Burant, S. S. Iyengar, J. Tomasi, M. Cossi, N. Rega, J. M. Millam, M. Klene, J. E. Knox, J. B. Cross, V. Bakken, C. Adamo, J. Jaramillo, R. Gomperts, R. E. Stratmann, O. Yazyev, A. J. Austin, R. Cammi, C. Pomelli, J. W. Ochterski, R. L. Martin, K. Morokuma, V. G. Zakrzewski, G. A. Voth, P. Salvador, J. J. Dannenberg, S. Dapprich, A. D. Daniels, O. Farkas, J. B. Foresman, J. V. Ortiz, J. Cioslowski and D. J. Fox, Gaussian, Inc., Wallingford CT, 2009.
32. D. McQuarrie, *Statistical Mechanics*, Harper & Row, New York, 1986.
33. A. V. Marenich, C. J. Cramer and D. G. Truhlar, *J Phys Chem B*, 2009, 113, 6378-6396.
34. J. M. Ho, A. Klamt and M. L. Coote, *J Phys Chem A*, 2010, 114, 13442-13444.
35. S. C. L. Kamerlin, M. Haranczyk and A. Warshel, *Chemphyschem*, 2009, 10, 1125-1134.

View Article Online
DOI: 10.1039/C3OB40988K

ToC Graphic

Hydroxylamine reacts with the diester anion DPP⁻ by the expected concerted S_N2(P) mechanism, but the reaction with the triester TPP involves an addition-elimination process, with the breakdown of the phosphorane intermediate rate-determining.

